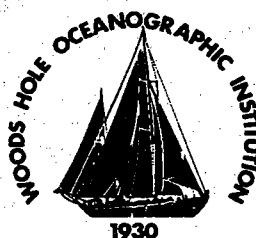


# Woods Hole Oceanographic Institution

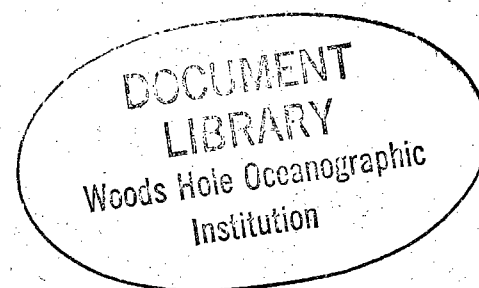


---

## Advanced Engineering Laboratory Project Summaries 1992

Edited by  
Daniel E. Frye

May 1994



## Technical Report

Funding was provided by the Woods Hole Oceanographic Institution.

Approved for public release; distribution unlimited.

---

**WHOI-94-14**

**Advanced Engineering Laboratory  
Project Summaries 1992**

Edited by  
Daniel E. Frye

Woods Hole Oceanographic Institution  
Woods Hole, Massachusetts 02543

May 1994

**Technical Report**



Funding was provided by the Woods Hole Oceanographic Institution.

Reproduction in whole or in part is permitted for any purpose of the United States Government. This report should be cited as Woods Hole Oceanog. Inst. Tech. Rept., WHOI-94-14.

Approved for public release; distribution unlimited.

**Approved for Distribution:**

A handwritten signature in black ink, reading 'George V. Frisk', is written over a horizontal line.

George V. Frisk, Chair  
Department of Applied Ocean Physics and Engineering

## **ABSTRACT**

The Advanced Engineering Laboratory of the Woods Hole Oceanographic Institution is a development laboratory within the Applied Ocean Physics and Engineering Department. Its function is the development of oceanographic instrumentation to test developing theories in oceanography, and to enhance current research projects in other disciplines within the community. This report summarizes recent and ongoing projects performed by members of this laboratory.

## **ARCTIC UNDER-ICE SURVEY OPERATIONS**

**James G. Bellingham, Max Deffenbaugh, John J. Leonard,  
Josko Catipovic and Henrik Schmidt . . . . . 5**

## **LASER SLOPE GAUGE LENS DESIGN AND OPTIMIZATION FOR SMALL SURFACE WAVE MEASUREMENTS**

**Erik Bock and Robin Singer . . . . . 6**

## **ROBUST MULTIUSER COMMUNICATION FOR UNDERWATER ACOUSTIC CHANNELS**

**David Brady and Josko Catipovic . . . . . 10**

## **THE ANNUAL EVOLUTION OF GEOSTROPHIC FLOW IN THE GULF OF MAINE: 1986-87**

**Brown, W. S. and J. D. Irish . . . . . 11**

## **INTEGRATED CTD OCEANOGRAPHIC DATA COLLECTION PLATFORM**

**Alan J. Fougere, Neil L. Brown, Edward Hobart . . . . . 12**

## **TELEMETRY CONCEPTS FOR DEEP SEA MOORINGS**

**Daniel E. Frye and Henri O. Berteaux . . . . . 13**

## **NOISE TESTS ON THE VALIDYNE DIFFERENTIAL PRESSURE SENSOR - Technical Memorandum**

**John T. Hallinan . . . . . 14**

## **REAL-TIME TELEMETRY IN THE GULF OF MAINE**

**J. D. Irish . . . . . 22**

## **SOLAR-POWERED, TEMPERATURE/CONDUCTIVITY/DOPPLER PROFILER MOORINGS FOR COASTAL WATERS WITH ARGOS POSITIONING AND GOES TELEMETRY**

**Irish, J.D., K. E. Morey and N. R. Pettigrew . . . . . 23**

**TECHNOLOGY FOR THE MEASUREMENT OF OCEANIC  
LOW FREQUENCY ELECTRIC FIELDS**

**Robert A. Petitt, Jr., Jean H. Filloux, and Alan D. Chave . . . . . 24**

**AN ALGORITHM FOR MULTICHANNEL COHERENT DIGITAL  
COMMUNICATIONS OVER LONG RANGE UNDERWATER ACOUSTIC  
TELEMETRY CHANNELS**

**Milica Stojanovic, Josko Catipovic and John Proakis . . . . . 26**

**ANALYSIS OF THE PERFORMANCE OF A DECISION FEEDBACK EQUALIZER  
ON FADING MULTIPATH CHANNELS IN THE PRESENCE OF  
CHANNEL ESTIMATION ERRORS**

**M. Stojanovic, J. G. Proakis and J. Catipovic . . . . . 27**

**THE AUTONOMOUS BENTHIC EXPLORER (ABE):  
A DEEP OCEAN SCIENTIFIC AUV FOR SEAFLOOR EXPLORATION**

**Dana R. Yoerger, Albert M. Bradley, and Barrie B. Walden . . . . . 28**

**THE PROGRAM TO TRACE THE DOS SYSTEM TIME CLOCK**

**Jia Qin Zhang and Warren E. Witzell, Jr. . . . . 30**

# **ARCTIC UNDER-ICE SURVEY OPERATIONS**

**James G. Bellingham, Max Deffenbaugh, John J. Leonard,  
Josko Catipovic and Henrik Schmidt**

## **ABSTRACT**

This paper describes the challenges of designing an autonomous underwater vehicle system for surveying the underside of the Arctic ice canopy. The operations are in support of an Arctic sea ice mechanics research program sponsored by the Office of Naval Research. The objective is to launch and recover an autonomous underwater vehicle through the ice to make measurements of the topography of the underside of the ice canopy. Transits of up to ten kilometers and mapping operations over an area of one square kilometer are desired. The vehicle, a modified version of the Odyssey AUV, is presently under construction and will be operated in the Arctic in spring of 1994.

Funding was provided by Office of Naval Research under contract N00014-92-J-1287 and the Massachusetts Institute of Technology Sea Grant College Program under contract NA90AA-D-SG424.

Published in: Proceedings 7th International Symposium on Unmanned Untethered Submersible Technology, University of New Hampshire, September 1991.

# **LASER SLOPE GAUGE LENS DESIGN AND OPTIMIZATION FOR SMALL SURFACE WAVE MEASUREMENTS**

**Erik Bock and Robin Singer**

## **ABSTRACT**

A lens design program has been written to optimize the detector of a laser wave-slope gauge, built at W.H.O.I. and tested in lab and field experiments. The gauge determines the two dimensional spectra of waves on the surface of the ocean. Careful detector design can minimize systematic errors and increase the accuracy of local surface slope measurements.

The gauge makes use of a laser light source that scans the water surface. The laser beam is deflected by refraction through the water-air interface where the local surface slope varies owing to the presence of waves. Once the beam is deflected, the optical receiver resolves the amount of deflection by determining the two orthogonal components of angular deflection.

The main errors introduced into the measurement scheme include the system's sensitivity to the relative distance between the water surface and the detector, nonlinearities intrinsic to the beam-sensing electronics, and asymmetries associated with the fact that the origin of the deflected beam is not on the optical axis of the system. Lens simulation software, that specifies the performance of an aspheric lens by means of exact ray tracing techniques, has been developed to minimize the error introduced by these effects. An optimal lens is designed by randomly altering the lens surfaces until the lens performance minimizes a set of error parameters derived as a measure of the systematic errors described above.

## **Motivation**

Laser slope gauges are routinely used to measure the small-scale wave structure associated with short water-surface waves. These waves are capillary and capillary-gravity waves (ripples) that have characteristics that are modified by oceanographic processes, including marine surfactant, subsurface currents, and variations in wind stress. Slope gauges rely on the refraction of a pencil-like laser beam at a point at the air-water interface that has a local slope owing to the presence of a wave. The amount of angular refraction can be related to the quantity-of-interest (i.e. the water slope) through Snell's law, given as:

$$n_1 \sin \theta_1 = n_2 \sin \theta_2$$

where  $n_1$  is the index of refraction of water,  $n_2$  is the index of refraction of air,  $\theta_1$  is

the angle between the incident laser beam and the surface normal of the air-water interface and  $\theta_2$  is the angle between the refracted beam and the surface normal of the interface. It is then convenient to measure the amount of angular refraction of the laser beam as it passes through the air-sea interface.

In the simplest case consider a water surface that has above it, a fixed flat screen that is in a plane parallel to the mean water surface. For low-amplitude waves, the location of the beam, after it has traveled away from the water surface and hit the screen, serves as an adequate approximation for the instantaneous local slope. When wave heights become significant, this simple approximation becomes invalid, because the distance between the water surface and the screen varies.

Since the small waves of interest (waves with wavelengths from a few millimeters to tens of centimeters) ride on the larger waves that can have wavelengths of tens of meters and amplitudes of several meters or more, we make use of a floating platform to deploy our slope gauge. The platform (a 6 m research catamaran named LADAS) follows the ocean surface so that the instrument mounted at the bow of the catamaran stays within 60 cm of the ocean surface. The detector is operated on the air-side of the interface. It makes use of an aspheric lens, designed with the first generation of the software described in this paper, to reduce errors associated with the residual height variations resulting from imperfect wave-following on the part of the catamaran.

### **Instrument description**

The instrument makes use of an aspheric lens, an optical scattering element, and analog detection electronics to determine laser deflection in the range of  $\pm 13$  degrees, with the origin of deflection varying in distance from the detector. The nominal distance between the water surface and the detector is 60 cm ( $\pm 30$  cm). The instrument was successfully deployed in several laboratory and field experiments here at Woods Hole, at the Canada Centre for Inland Waters (CCIW), and off Cape Hatteras as part of the High Resolution ARI pilot and main field experiments.

### **Lens design software**

The software was written to find an optimal lens with minimal spread and linear errors, as defined below. These error values indicate the accuracy of the optical systems:

Spread error is defined as the sum of the standard deviations of the distances,  $r$ , at the focal plane, from its center (the optical axis), of rays of differing incidence angle,  $\theta$ , that had origin at different starting distances,  $z$ , from



the lens and at different orientation angles,  $\phi$ . Formally, it is defined as:

$$\frac{1}{n_{\theta}} \times \sum_{\theta=0}^{\theta_{\max}} \sqrt{\frac{1}{n_{\phi z}} \times \sum_{\phi=0}^{2\pi} \sum_{z=z_{\min}}^{z_{\max}} (r - \mu_r)^2}$$

where  $\mu_r$  is the mean of the  $r$  values,  $n_{\phi z}$  is the number of rays per incident angle, and  $n_{\theta}$  is the number of incident angles.

Linear error is defined as 1 minus the regression coefficient for the same set of rays using the linear regression between distance from center at the focal plane,  $r$ , and the angle of incidence,  $\theta$ ; it is given as:

$$1 - \left[ \frac{1}{n_{\theta}} \times \sum_{\theta=0}^{\theta_{\max}} \left( \frac{m_{r\theta} - \overline{m_{r\theta}}}{\sigma_m} * \frac{\theta - \overline{\theta}}{\sigma_{\theta}} \right) \right]$$

where  $m_{r\theta}$  is the mean of the distances ( $r$ ) for a given angle  $\theta$ , and  $\overline{m_{r\theta}}$  is the mean of those means,  $\sigma_m$  is the standard deviation of the means,  $\overline{\theta}$  is the mean of the angles,  $\sigma_{\theta}$  is the standard deviation of the angles, and  $n_{\theta}$  is the number of incident angles.

Spread error is proportional to the degree of scatter of the rays, and linear error is proportional to the nonlinearity of the relation between incoming angle and the amount of displacement at the focal plane.

The program starts by reading a lens data file, which contains the coefficients of two twelfth order polynomials that describe the upper and lower surfaces of a lens, the working focal length which is allowed to vary in the current strategy, and the previously calculated best value of spread error and linear error. Two of the lens coefficients are randomly permuted in order to describe a new lens. The new lens must pass a set of tests in order to determine if it is physically realizable and if it is, rays are traced through the new lens to a set of positions on the focal plane. This enables the calculation of spread and linear errors which are used for determining the accuracy of the optical system.

If either error value is lower than the recorded error values for the previous lens, the lens coefficients and focal length are written to a data file along with the improved error value. Lens parameters producing a better spread error are used for future iterations. The range of distances and the ranges of incident angle and orientation are all specified by the lens designer. The ray tracing is accomplished in three dimensional geometry, using the three dimensional extension of the Newton-Raphson method for finding intercepts, and applications of Snell's Law. The spread error calculation is based on the standard deviation of the universe, not the sample standard deviation. The minimum and maximum lens thickness, the lens' radius, and the index of refraction are specified as constants and can be easily modified. A modification of this code and some Matlab "M" files permit the generation of plots of the locations at which the rays strike the focal plane. These plots enable the lens designer to evaluate the performance of the lens, and to determine when an acceptable design has been achieved.

### **Software use**

The code has been used on a 20 MHz 386 PC and will converge to an optimized lens in an overnight run. The optimized parameters in the data file can be used as specifications to Applied Products Corporation, located in Bristol, Pennsylvania, who can machine an acrylic lens from them. For use in the laser-slope gauge, the lens is covered with a tinted (red) acrylic plate and the contact area between the plate and lens is oil-filled with silicone fluid to match the index of refraction and prevent satellite reflections at multiple air/acrylic interfaces.

After a new lens has been chosen, it will be fabricated and tested with lasers in the laboratory to evaluate its performance. It is anticipated that it will be incorporated in laboratory experiments in Heidelberg, Germany in October of 1994, and in future field experiments.

### **Conclusion**

By simulating the path of rays through randomly generated, simulated lenses, a lens can be found that improves the performance of a limited range laser-slope gauge. This will aid in the characterization of the capillary and capillary-gravity waves at the surface of the ocean.

Funding was provided by Office of Naval Research under Contract N00014-90-J-1717.

# **ROBUST MULTIUSER COMMUNICATION FOR UNDERWATER ACOUSTIC CHANNELS**

**David Brady and Josko Catipovic**

## **ABSTRACT**

This paper presents a method for easing acoustic channel congestion present whenever multiple acoustic systems or multiple UUVs are sharing acoustic bandwidth. We consider the acoustic environment as a multiuser network, where multiple systems (users) need to operate synchronously, with minimal regard for other channel users. In many multipoint random access networks, the collision of data packets from two co-channel and asynchronous transmitters is viewed as unresolvable. Network protocols are usually designed to avoid and discard packet collisions, and to utilize a side channel for retransmission requests to both transmitters. This paper presents a random-access communication network capable of resolving collisions between several asynchronous and co-channel packets without side channel communication.

The algorithm differs from standard capture schemes by demodulating the data from both strong and weak transmitters. The resulting acoustic network protocol requires roughly the same transmission bandwidth as other networks at the expense of an increased computational complexity at the receiver processor. Examples are given and illustrate that this technique is extremely desirable for underwater acoustic local area networks and underwater autonomous vehicles with both side-scan sonar as well and acoustic telemetry links.

Funding was provided by National Science Foundation under Contract OCE92-01191.

Published in Proceedings IEEE Unmanned Underwater Vehicle Conference, June 1992.

# **THE ANNUAL EVOLUTION OF GEOSTROPHIC FLOW IN THE GULF OF MAINE: 1986-87**

**Brown, W. S. and J. D. Irish**

## **ABSTRACT**

The evolution of geostrophic flow in the Gulf of Maine has been documented using five water property surveys conducted during the thirteen-month period of moored observations in 1986-1987. The scales of mesoscale flow decreased from 100-200 km during winter to 50-100 km in late summer - apparently related to an evolving water mass structure. The basin-scale geostrophic transport around Jordan Basin underwent several reversals during the year, ending with a weak counterclockwise Gulf of Maine gyre in September 1987.

Published in Journal of Physical Oceanography, 22(5), 445-473, 1992

Funding provided by National Science Foundation under contract OCE 8818060 and NOAA Sea Grant Program.

# **INTEGRATED CTD OCEANOGRAPHIC DATA COLLECTION PLATFORM**

**Alan J. Fougere, Neil L. Brown, Edward Hobart**

## **ABSTRACT**

The Mark II conductivity-temperature-depth (CTD) profiler has been a mainstay of modern physical oceanographic research. The MKIIIB CTD provides high quality oceanographic data when used by skilled personnel and require frequent recalibration. The design objective of the Integrated CTD system was to attain the same high level of performance while reducing the necessity of frequent recalibration through the enhancement of long term stability. This goal required consideration of both the electronic approach and the re-design of the physical sensors. The result of this work is a CTD system with improved measurement precision. All three primary sensors are newly designed to achieve long term measurement stability and to optimize system sampling performance without the limitations of existing technologies.

Advances in the state of the art in electronic and microcontroller technologies has enabled the development of improved methods of analog sensor signal processing. The revolution in high speed microcontrollers has allowed their use in the Integrated CTD allowing for real time numerical correction for drift in the analog signal processing circuitry.

Funding provided by Woods Hole Oceanographic Instrument Initiative under project #33423300.

Published in Proceedings Oceanology International '92, Brighton, England, March 1992.

# TELEMETRY CONCEPTS FOR DEEP SEA MOORINGS

Daniel E. Frye and Henri O. Berteaux

## ABSTRACT

To expand the state of the art in moored array technology, Woods Hole Oceanographic Institution (WHOI) is pursuing a series of engineering tests conducted from buoys moored offshore Bermuda. Assessment of new sensors and data transmission techniques are included in the evaluation of new buoy and mooring components of markedly improved performance as are measurement of buoy system dynamics, and long term exposure of new materials.

Reasons for selecting Bermuda as the test site included proximity to deep water, the facilities for staging and monitoring the experiment (Bermuda Biological Station for Research), an abundance of winter storms and an occasional hurricane, a good collection of epipelagic and mesopelagic predators, and availability of the R/V Weatherbird. The site duplicates the hostile conditions encountered in many other remote parts of the Atlantic.

The experimental work involves the long-term (18 month or more) exposure of components and a systematic evaluation of their performance in situ. Degradation due to corrosion, fatigue, fouling, fishbites, etc., is carefully monitored as a function of depth and time.

Results of the engineering surface oceanographic mooring (ESOM) experiment in 1989-1990 were discussed in *Sea Technology* (February 1992). ESOM was also used as a platform from which to conduct the full-scale, in situ evaluation of an underwater acoustic telemetry system developed by Dr. Josko Catipovic and engineers in the Advanced Engineering Laboratory at WHOI (*Sea Technology*, May 1990).

A second experimental mooring, ALTOMOOR (Atlantic long term oceanographic mooring), will be deployed offshore Bermuda in 1993. In addition to the continued testing of moored array components, this mooring will be used to acquire a comprehensive set of mooring dynamic measurements, to assess the performance of a new acoustic current meter developed by Neil Brown of WHOI and finally to evaluate inductive coupling techniques for underwater telemetry.

Funding provided by Office of Naval Research. Moored Array Technology is supported by Dr. S. Ramberg, director of the Ocean Engineering Division, contract No. N00014-90-J-1719. Telemetry development was supported by Dr. D. Evans under contract No. N00014-86-K-0751.  
Published in *Sea Technology*, May 1992.

# NOISE TESTS ON THE VALIDYNE DIFFERENTIAL PRESSURE SENSOR - Technical Memorandum

John T. Hallinan

Several tests were carried out in order to determine if the Validyne DP15-34 Differential Pressure Sensor is capable of resolving 10 Pascal while maintaining a full scale capability of 22,000 Pascal. The 16 bit AtoD and the 4 Pole low pass filters from the ONR OBS were used to make the measurements. Figure 1 describes the setup.

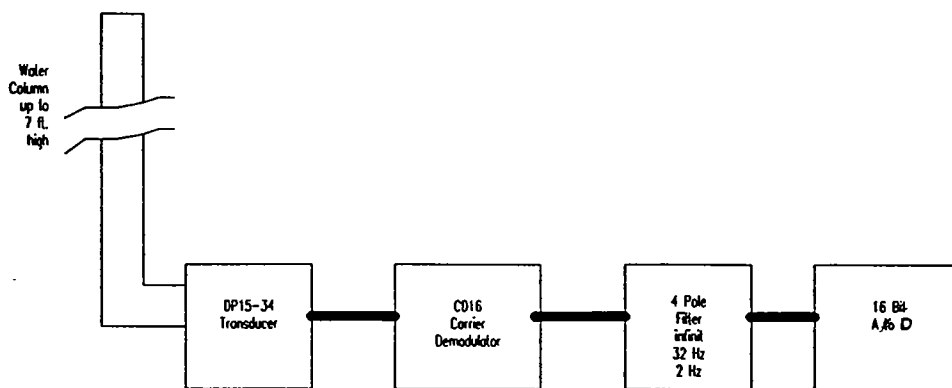


Figure 1

The plotting program is described below.

1. The plot program determines the maximum and minimum values in the data set that it will plot and compresses the vertical scale so the wave form fills the complete screen. It does this for each iteration of the plot and when the zoom feature is used the scale will change.
2. The program compresses the horizontal scale so that the data set fills the full screen. The zoom feature will also change this scale.

3. The numbers in the upper right corner of the plot are the maximum and minimum values contained in the data set. The units are number of LSBs of the 16 Bit Bipolar AtoD. The full scale range is 32767 to 32768. The program prints the maximum and the minimum values and computes the difference to plot the peak to peak value.
4. A conversion factor of  $.000146/lb \cdot in^{-2} = 1Pa$  is used in the calculations.
5. The system was calibrated by raising the height of the water in the water column approximately seven feet above the transducer and adjusting the span of the CD16 to give five Volts input to the AtoD.

Fresh water was used which has a density of  $62.4/lb \cdot ft^{-3}$ .

$$62.4/lb \cdot ft^{-3} \div 144in^2 \cdot ft^2 = .433333lb \cdot ft^{-1} \cdot in^{-2}$$

$$22,000 Pa \times .000146/lb \cdot in^{-2} \cdot Pa^{-1} = 3.212lb \cdot in^{-2}$$

$$3.212lb \cdot in^{-2} \div .433333lb \cdot ft^{-1} \cdot in^{-2} = 7.41ft$$

which means that the full scale reading of the AtoD, 32767 LSBs is approximately 22 KPa and each bit has a weighting of 0.671387uPa

$$22,000Pa \div 32,768Bits = 0.671387Pa \cdot Bit^{-1}$$

The Validyne Carrier Demodulator CD16 furnishes a 5 KHz square wave to the DP15-34 transducer to excite the coils and the CD16 demodulates the transducer signal to a DC output. Therefore there is a high probability that the 5 KHz will find its way into the data. The first test set the 4 pole filter pass band to infinity (i.e. no filter), the level of the water in the water column was zero inches, the sample rate was 128 samples per second. Figure 2 is a plot of the data collected. Independent readings from an oscilloscope showed the 5 KHz was riding on the analog signal but that the level was on the order of 7 mV peak to peak which is within the ripple specification for the CD16. Figure 2 shows the effect of the 5 KHz beating against the 128 Hz Sample rate.

The data in Figure 2 has a peak to peak pressure differential of  $455 Bits \times 0.671387Pa \cdot Bit^{-1} = 305.5Pa$ .



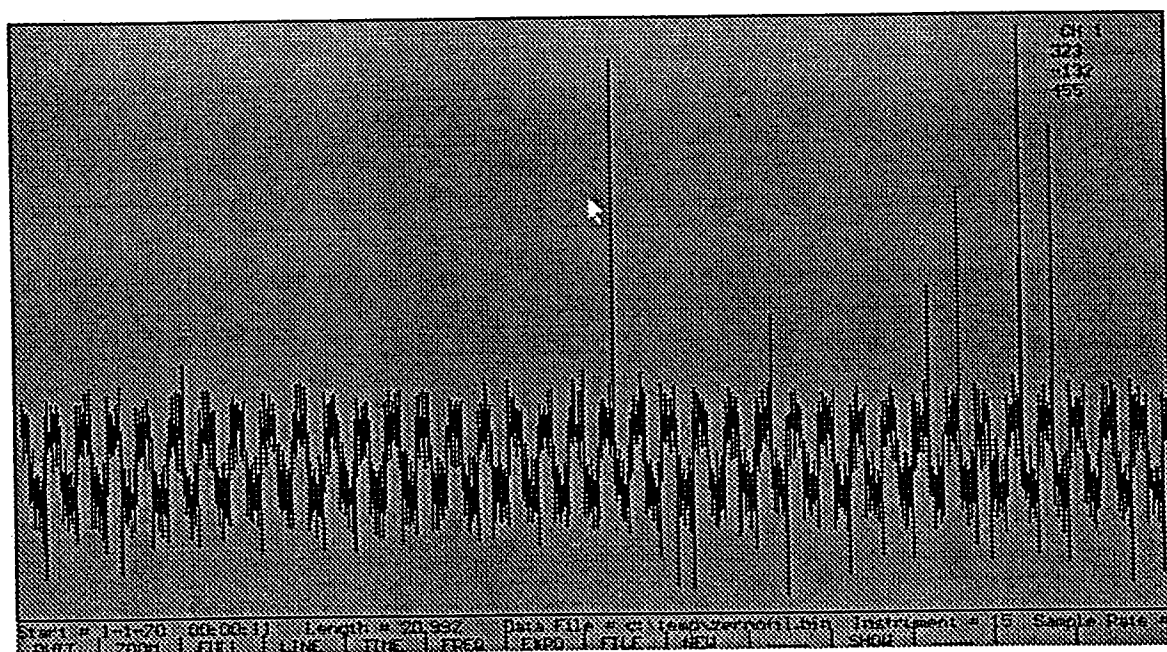


Figure 2

However, this differential is skewed by several single sample spikes. Figure 3 shows a zoomed plot of the same wave form without the spikes. This section of data has a peak to peak differential of  $143\text{Bits} \times 0.671387\text{Bits} \cdot \text{Pa}^{-1} = 96\text{Pa}$ , which is ten times as much as we are trying to resolve.

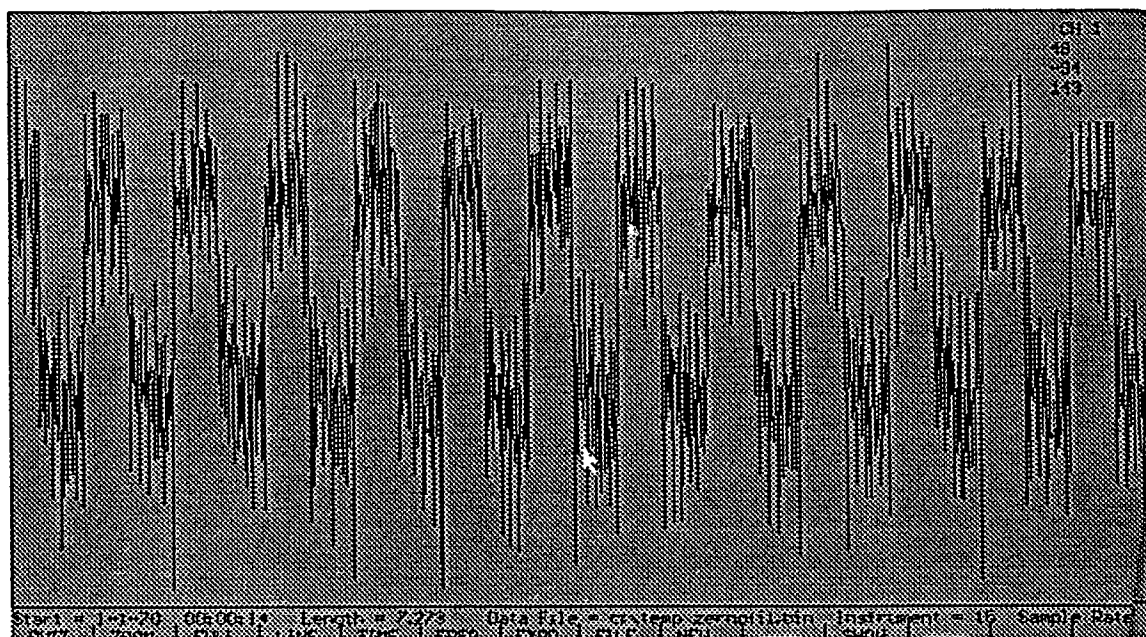


Figure 3

In the second test the 4 pole low pass filter was set to 32 Hz. The independent oscilloscope wave form did not show the 5 KHz. The water level was set to approximately zero inches. Figure 4 is a plot of the data collected.

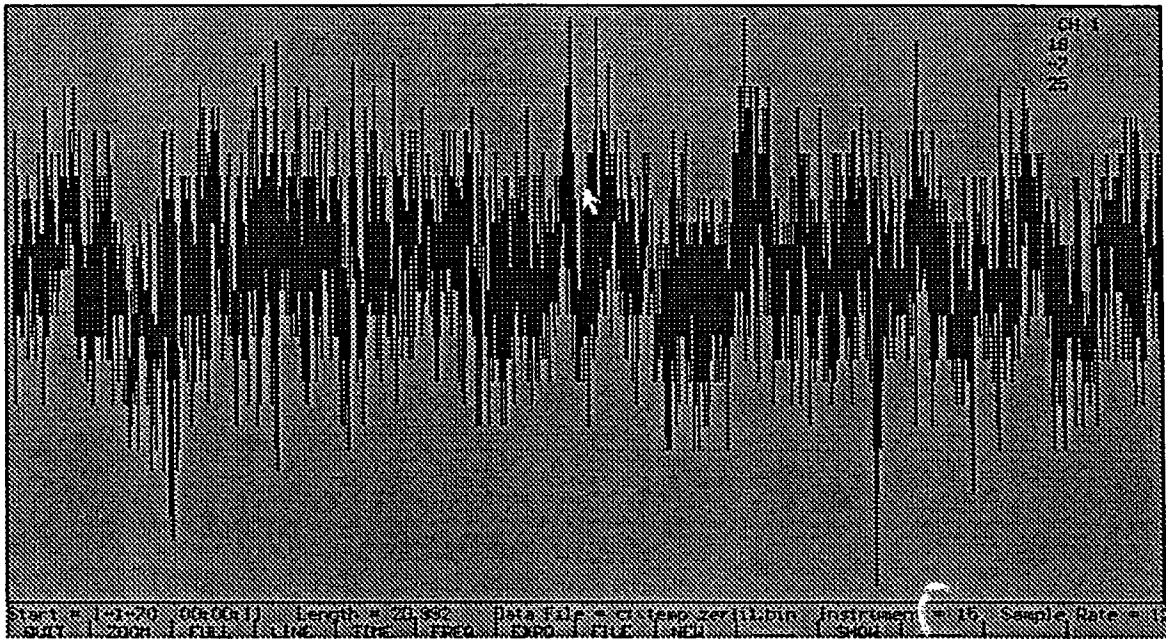


Figure 4

The peak to peak magnitude of this data is  $25\text{Bits} \times 0.671387\text{Pa} \cdot \text{Bit}^{-1} = 16.78\text{Pa}$  which is the ball park of the 10 Pa we would like to resolve.

In the third test the low pass filter was set to 32 Hz, the sample rate was 128 samples per second and the water column was raised to approximately seven feet as smoothly as the human hand could move and then lowered to zero inches

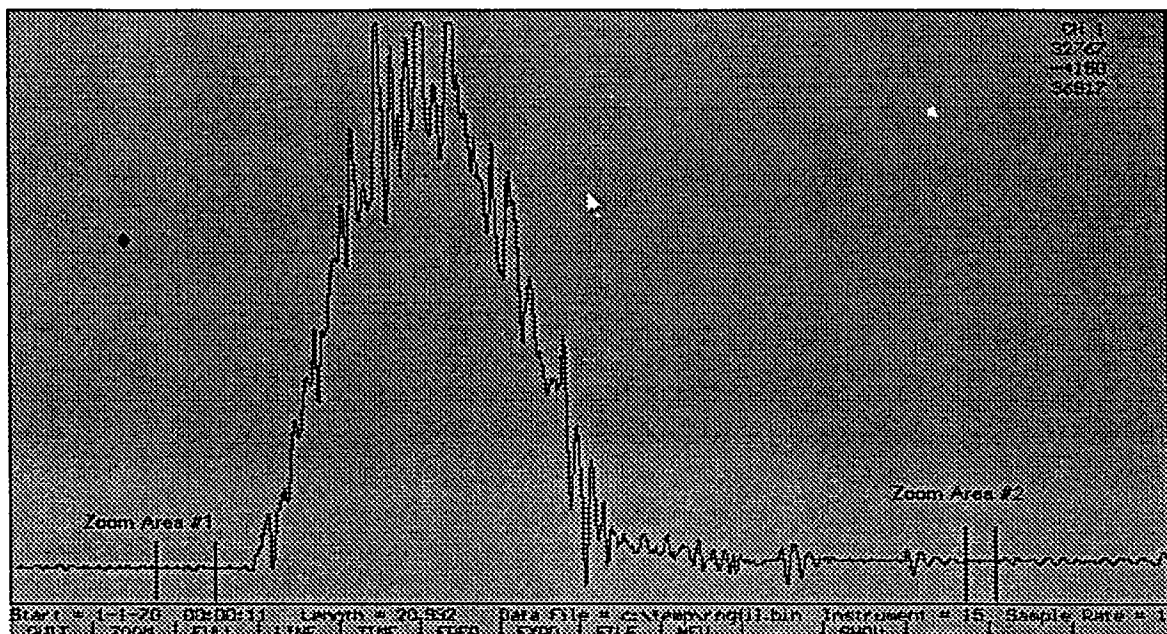
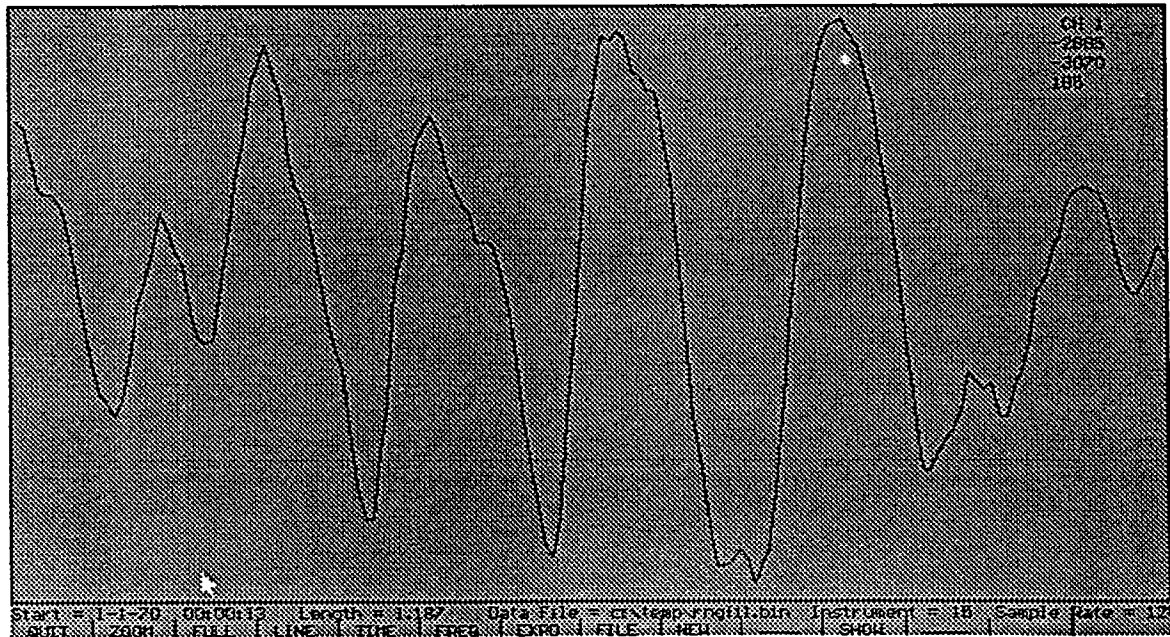
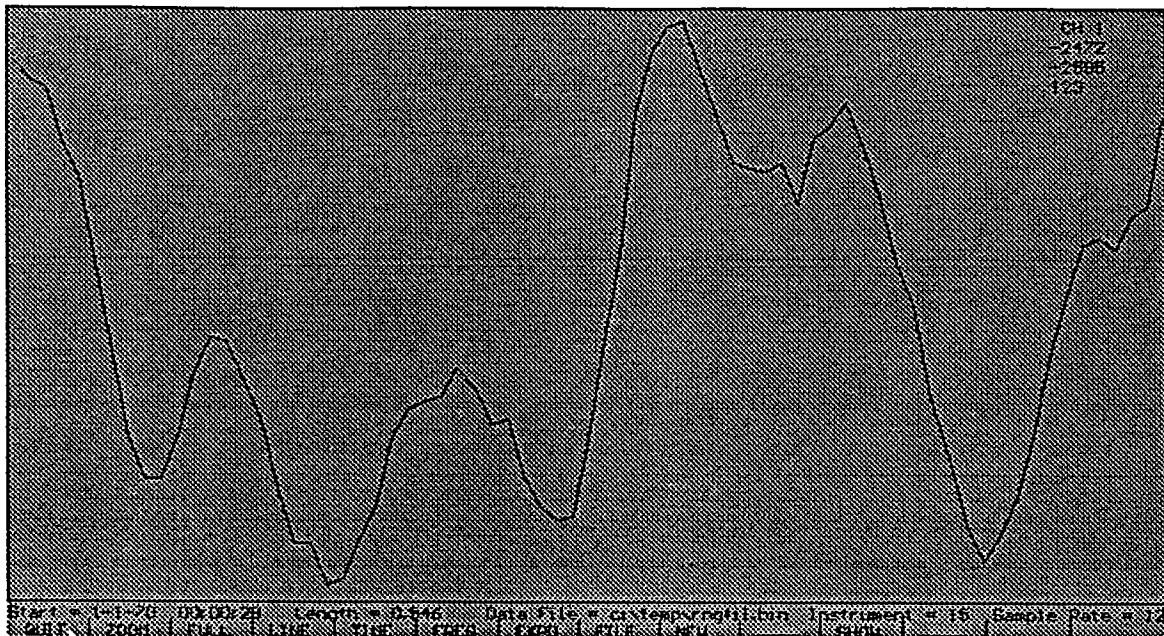


Figure 5

Clearly we are able to measure 22 KPa. To get some sense of the background noise two zoom areas, zoom area #1 and zoom area #2, were selected and are plotted below.



Zoom area #1 shows a peak to peak magnitude of  $185\text{Bits} \times 0.671387\text{Pa} \cdot \text{Bit}^{-1} = 124.2\text{Pa}$



Zoom area #2 shows a peak to peak magnitude of  $123\text{Bits} \times 0.671387\text{Pa} \cdot \text{Bit}^{-1} = 82.58\text{Pa}$

Given the noise levels in Figure 4, the levels in Zoom areas #1 and #2 probably reflect the motion of the water due to the activity of moving and positioning the water column.

In test four, the low pass filter was set to two Hertz, the sample rate was 128 samples per second and the height of the water column was approximately zero inches. The data is plotted in Figure 6. The peak to peak magnitude is  $24\text{Bits} \times 0.671387\text{Pa} \cdot \text{Bit}^{-1} = 16.11\text{Pa}$ .

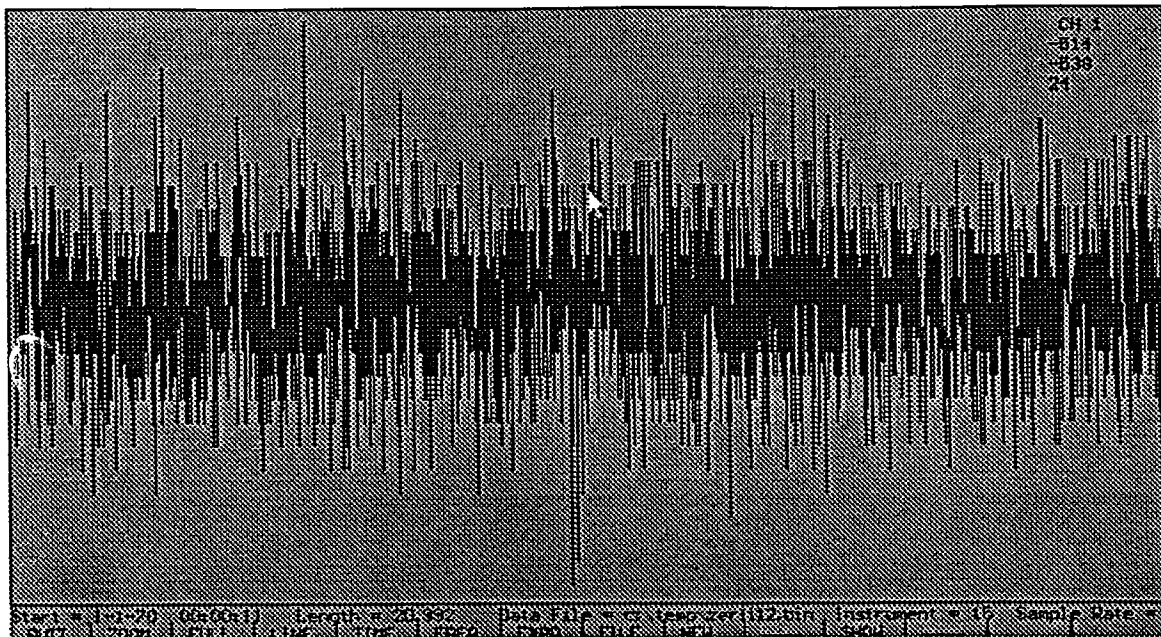


Figure 6

In test five the low pass filter was set to two Hertz, the sample rate was 128 samples per second, the water column was raised smoothly from zero inches to seven feet and back to below zero inches. Figure 7 is a plot of the test five data set. Again, the system is capable of measuring 22 KPa and two zoom areas, zoom area #3 and zoom area #4, have been plotted to determine the background noise. The peak to peak magnitude of the data in zoom area #3 is  $16\text{Bits} \times 0.671387\text{Pa} \cdot \text{Bits}^{-1} = 10.74\text{Pa}$ .

The data set in Zoom area #4 needs further refinement and Zoom area #5 is that refinement.



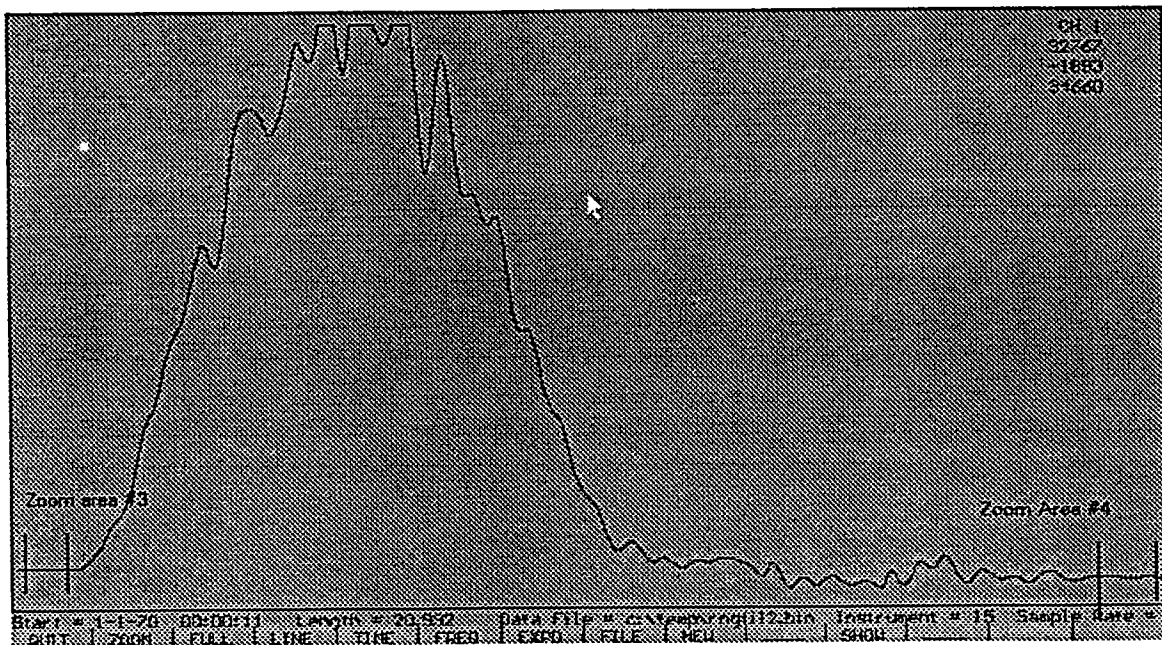
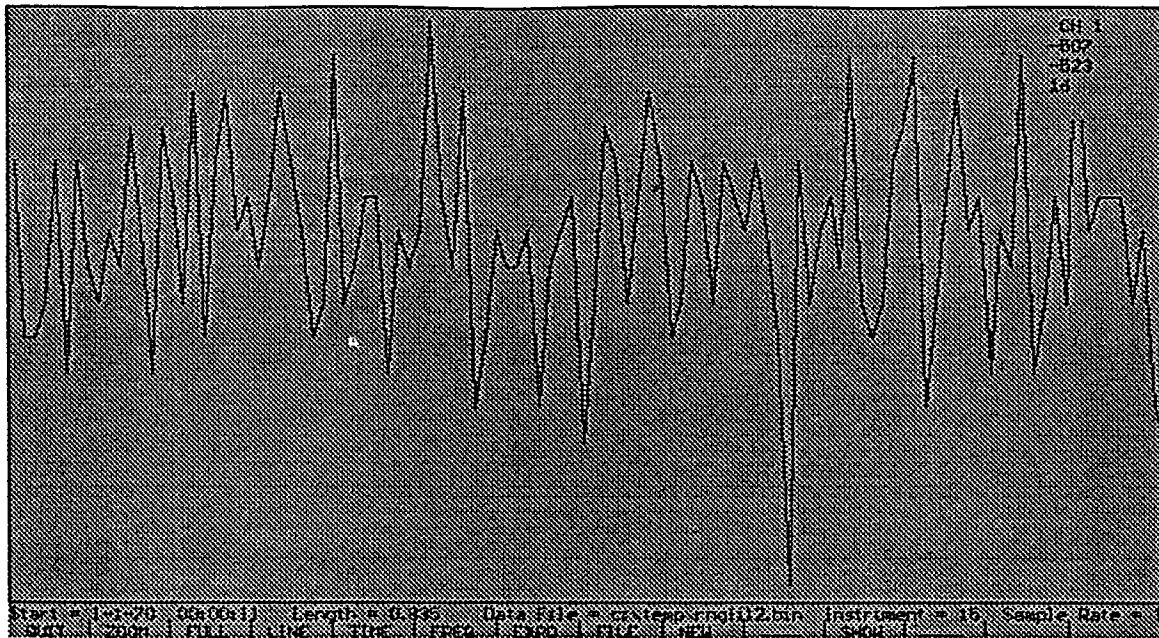
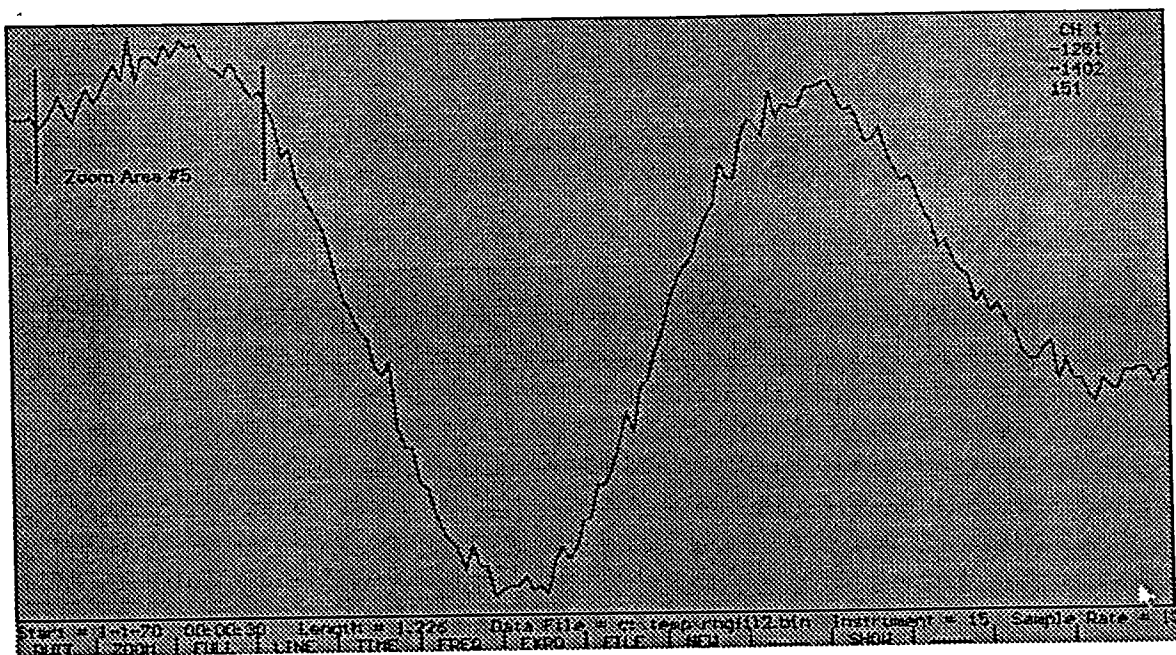


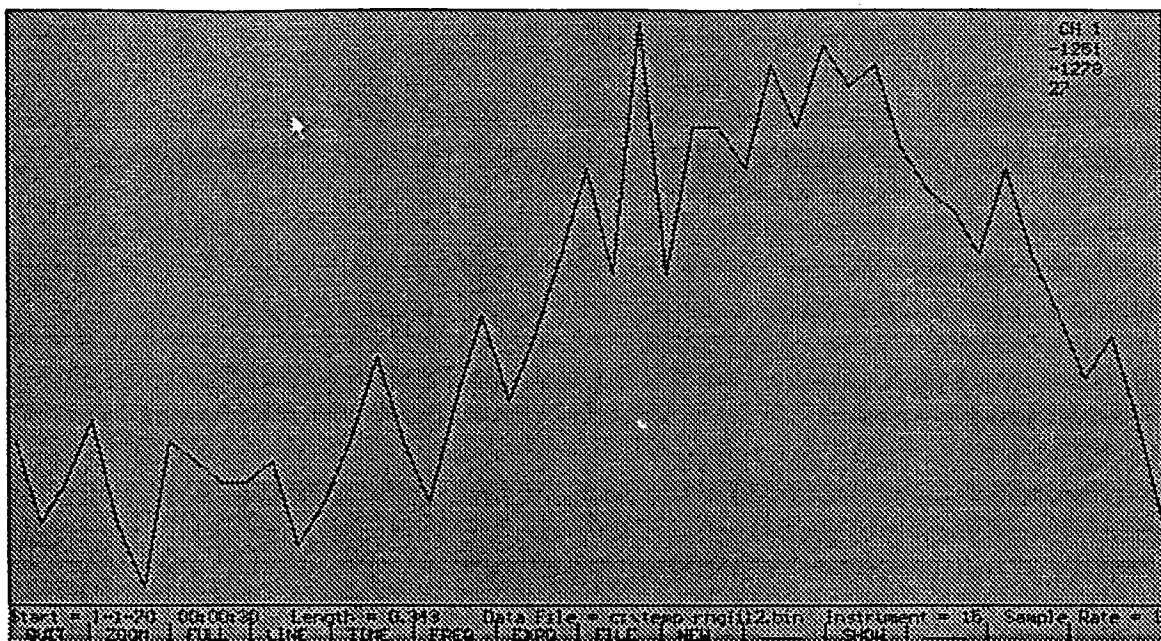
Figure 7



Zoom Area #3



**Zoom Area #4**



**Zoom Area #5**

The peak to peak magnitude of data in zoom area #5 is  $27\text{Bits} \times 0.671387\text{Pa}$ .

$\text{Bit}^1 = 18.13\text{Pa}$ .

Clearly 10 Pa is discernible in this plot and the conclusion is that the Validyne DP15-34 Differential Pressure Sensor coupled with the appropriate low pass filter and 16 bit AtoD will give us the resolution and the range we want.

Funding provided by National Science Foundation under Contract OCE 91-16601.

# **REAL-TIME TELEMETRY IN THE GULF OF MAINE**

**J. D. Irish**

## **ABSTRACT**

In the Gulf of Maine, the University of New Hampshire is utilizing several telemetry schemes to return data and diagnostics from remote instrumentation. Data collecting platforms with GOES transmitters on solar powered surface buoys are used to return temperature and conductivity time-series from vertical arrays below the buoy. ARGOS is used for positioning these surface buoys and for a back-up data telemetry link. UNH is also developing pop-up data capsules to relay data from bottom instruments which also act as surface drifters. Most recently, the GOES data system is being used to monitor the operation of an acoustic Doppler current profiler mounted on a surface buoy. In near-shore regions, packet radio technology makes two-way, error-free communications possible, and acoustic links are under development to connect bottom instruments to the UNH surface buoys.

Published in Proceedings of the Gulf of Maine Scientific Workshop, Woods Hole, MA, January 8-10, 1991, ed. J. Wiggin & C.N.K. Mooers, 251, 1992

Funding provided by National Science Foundation under Contract OCE8818060 and NOAA Sea Grant.



# **SOLAR-POWERED, TEMPERATURE/CONDUCTIVITY/DOPPLER PROFILER MOORINGS FOR COASTAL WATERS WITH ARGOS POSITIONING AND GOES TELEMETRY**

**Irish, J.D., K. E. Morey and N. R. Pettigrew**

## **ABSTRACT**

Over the past 12 years we have developed and refined instrumented surface buoy systems for our coastal research programs. A buoy consists of a steel ball on which are mounted solar panels, an electronics and battery housing, a radar reflector, guard light and antenna. The system is moored by a Kevlar-core electromechanical cable with an elastic element at the bottom. A microprocessor-controlled data system switches the power to the sensors, digitizes the output, and transmits the data via GOES. An ARGOS link transmits diagnostic information, and the buoy's location in case it should break loose. Temperature and conductivity are measured at several depths along the mooring, and most recently currents were measured with a downward-looking Acoustic Doppler Current Profiler mounted just below the buoy. Deployments with various configurations have been made in the Gulf of Maine and Massachusetts Bay for periods up to 13 months. Our experience has shown that reliable moorings with telemetry are feasible for at least one year in coastal waters.

Published in Proceedings Oceans '92, Newport, RI, 730-735, October 28, 1992

Funding provided by National Science Foundation under Contract OCE-88-18060, NOAA/Sea Grant under Contract R/FM-104), Massachusetts Bays Program, USGS, and Woods Hole Oceanographic Institution proposal #8078.

# TECHNOLOGY FOR THE MEASUREMENT OF OCEANIC LOW FREQUENCY ELECTRIC FIELDS

Robert A. Petitt, Jr., Jean H. Filloux, and Alan D. Chave

## ABSTRACT

Low frequency ( $<0.01$  Hz) electric field data from the ocean have wide applications in basic research into the structure of the solid earth, in exploration geophysics, in studies of the depth-averaged velocity structure of ocean currents, and in tactical oceanography. However, a number of unique problems caused by the oceanic environment must be overcome to achieve stable measurements to frequencies as low as  $10^{-8}$  Hz. First, the high conductivity (3-5 S/m) of seawater results in substantially weaker electric fields in the ocean than in other geological materials. This means that precision, low noise electronics must be used and that even the faint field generated by corrosion of metallic parts may be capable of swamping the signal of interest. Second, even the best non-polarizing electrodes exhibit a time variable offset voltage which is often much larger than that produced by the external electric field. Finally, the very long period nature of oceanic electric field phenomena places extreme stability requirements on instrument electronics. None of these problems are as important for electric field measurements on land, and a very different approach is required in the ocean environment.

As a case history, this paper will describe instrumentation that has overcome these obstacles in a low power package capable of multi-year deployments in the deep ocean. The electric potential is measured between the ends of orthogonal, 3 m long pairs of seawater-filled plastic pipes or salt bridges. The inner ends of the salt bridge are connected to a mechanical DPDT fluid switch or water chopper which physically reverses the electrodes during the measurement cycle. As the switch changes position, a set of non-polarizing silver-silver chloride electrodes are alternatively connected to opposite ends of the salt bridge. This not only removes electrode drift, but eases the necessity for ultra stable analog electronics. After amplification by a low power differential amplifier, analog-to-digital conversion is achieved using a voltage controlled oscillator followed by a simple counter. A low power microcontroller handles all basic instrument functions including data storage in EEPROM memory. All of the electronics, including batteries, orientation compass, and a radio transmitter for recovery location, are contained in a single 17 inch glass sphere pressure case. The least count sensitivity of this instrument is

20 nV/m, corresponding to an electric potential of 60 nV across the 3 m salt bridge. Based on spectral analysis of seafloor records, the real instrument noise level is substantially lower than this figure. The baseline stability over long deployments is comparable.

Funding provided by National Science Foundation Contract OCE91-96235.

# **AN ALGORITHM FOR MULTICHANNEL COHERENT DIGITAL COMMUNICATIONS OVER LONG RANGE UNDERWATER ACOUSTIC TELEMETRY CHANNELS**

**Milica Stojanovic, Josko Catipovic and John Proakis**

## **ABSTRACT**

The problem of achieving reliable digital communications over long range underwater acoustic telemetry channels is addressed, and a receiver algorithm for multichannel coherent data detection is presented. The receiver consists of a  $T/2$  fractionally spaced bank of feedforward equalizers, a multichannel carrier phase synchronizer and a common decision feedback section of the equalizer. An adaptive algorithm is derived based on joint minimum mean squared error optimization of the receiver parameters. The equalizer tap coefficients and estimates of the carrier phases are updated using a combination of a recursive least squares algorithm and a second order multichannel digital phase locked loop. Since the equalizer accomplishes the function of symbol synchronization, no separate delay locked loops are necessary.

The algorithm is successfully applied to the experimental data. The results assert feasibility of coherently combining multiple arrivals in each of the diversity channels, and demonstrate additional spatial diversity improvement.

Funding was provided by Advanced Research Projects Agency under Contract MDA972-91-J-1004.

Published in Proceedings Oceans '92, Newport, RI, October 28, 1992, pp 577-582.

# **ANALYSIS OF THE PERFORMANCE OF A DECISION FEEDBACK EQUALIZER ON FADING MULTIPATH CHANNELS IN THE PRESENCE OF CHANNEL ESTIMATION ERRORS**

**M. Stojanovic, J. G. Proakis and J. Catipovic**

## **ABSTRACT**

A coherent receiver with an adaptive decision feedback equalizer (DFE) operating on a Rayleigh fading channel is considered. A common assumption in the analyses of a DFE is that the receiver has perfect knowledge of the channel impulse response. However, for a rapidly fading channel, errors in channel tracking can become significant. We analyze theoretically the impact of these errors on the performance of a multichannel DFE. The expression obtained for the achievable average PSK bit error probability depends on the estimation error co-variance. To specify this matrix, we focus on a special case when the Kalman filter is used as an optimal channel estimator. Conveniently, the bit error probability can be assessed directly in terms of the channel fading model parameters, the most interesting of which is the fading rate. Our results show the penalty imposed by imperfect channel estimate as well as the fading-induced irreducible error rates.

Funding provided by Advanced Research Projects Agency under Contract MDA972-91-J-1004.

# **THE AUTONOMOUS BENTHIC EXPLORER (ABE): A DEEP OCEAN SCIENTIFIC AUV FOR SEAFLOOR EXPLORATION**

**Dana R. Yoerger, Albert M. Bradley, and Barrie B. Walden**

The autonomous benthic explorer (ABE) is a vehicle that will perform scientific surveys of the seafloor over an extended period of time without a support vessel, complementing manned submersibles and ROVs. A preliminary application of ABE will be repeated surveys of hydrothermal vent areas at depths of 4,000 to 6,000 meters.

Hydrothermal vents are dynamic structures that occur in seafloor spreading regions along the Mid-ocean ridge where proximity of underlying magma drives an associated hydrothermal circulation. As the water exits the seafloor, it cools rapidly and deposits enormous amounts of solute, often in chimney structures as high as 10 meters.

The resultant fluxes of heat and chemicals directly effect the chemical and thermal balances of the entire ocean. The hydrothermal vents also fuel vibrant ecosystems through chemosynthesis. Diverse bacteria use the chemical energy from reduced compounds in the fluids to provide food for animal life. In turn, biological activity alters the vent fluids.

Better observations are required to answer many basic questions. The chemical flux from the vents may dominate and stabilize the global long-term composition of seawater or it may be trivial - it depends on what estimate of total flux is used, high or low. Plumes of the hot, buoyant fluids from the vents may also effect circulation on a basin-wide scale. Little is known about their temporal variability.

Manned submersibles will continue to play a dominant role, particularly for optical imaging studies and sampling. ROVs (towed and tethered) and specialized instruments lowered on cables will be used more in the future, with increased multi-sensor capabilities, high-bandwidth real-time feedback to the surface, and improved endurance. They will tend thermal, acoustic, optical, and micral instruments on the bottom or in moored arrays.

Expeditions by ROVs and submersibles cannot remain on a given site for more than a few weeks at a time or return to the site very often. On the other hand, ABE, over extended periods of time and independent of a support vessel, will capture the dynamics of the vent processes.

Complementing fixed instrumentation, ABE will provide "snapshots" taken at prescribed intervals over an area of several thousand square meters. ABE,

commanded to perform a survey by fixed instrumentation, will carry instruments that detect intersecting transient phenomena such as seismic events or releases of fluid, mitigating the need for a dense network of fixed sensors.

Dominant design considerations for ABE were that it function initially for about six weeks but eventually for a year on a mission and at depths to 6,000 meters. Number of sensors and volume of data was not to rival that of ROVs or manned submersibles, only to fill the gap between full-scale surveys. Specifications are: maximum speed - 2 knots; cruise speed - 1 knot; total survey distance - 30 kilometers; and total survey time - 50 hours.

Preliminary scenarios require the site to be prepared with acoustic beacons and an anchoring point by an ROV or submersible. ABE will be acoustically navigated, equipped with optical imaging sensors permitting precisely navigated photo surveys to be repeated, and be able to measure physical properties of seawater.

Funding by National Science Foundation under Contracts OCE-90-20227 and OCE-92-16775.

Published in: Sea Technology, January 1992, pp. 50-54

# THE PROGRAM TO TRACE THE DOS SYSTEM TIME CLOCK

Jia Qin Zhang and Warren E. Witzell, Jr.

The time stamps provided by the DOS system of a PC during the acquisition of data are subject to inaccuracies that we found unacceptable. We have written a program that allows for correction of these errors, using a reading from a precise clock generator as a reference.

The problem with the PC system time clock is the drift of the crystal frequency in the CMOS oscillator. This is aggravated by temperature changes when the PC is used outdoors; the time clock may drift irregularly, sometimes changing as much as several seconds within twenty-four hours.

There were two possible solutions to this problem which we investigated and rejected. A software solution would be to set the DOS time clock with a time clock station via a telephone modem receiver; this, however, gives an accuracy no better than one second. A hardware solution would be to maintain a separate time base circuit which has a high frequency stability in wide temperature ranges; in our situation, the use of this hardware is not feasible.

We chose a third solution. We wrote a program that uses the output from a precise time clock generator. This way we can set the DOS clock to an accuracy of 55ms, which is the smallest step by which a PC time clock can be changed. Using the program is both simple and efficient.

The only hardware required, in addition to the precise clock generator, is a coaxial cable to connect the printer strobe signal pin on the PC with the display-lock input of the clock generator. The program is written in C, using "SpontaneousAssembly for C/C++ Version 3.0", a C language library for optimizing C programs in assembly.

The program initially captures the PC system time and stores it in a buffer. At the same moment, it sets the strobe signal generator, which shows hour, minute, second, and hundredths of a second. On the PC the DOS time is displayed, so the user can see the difference between the two clock readings. The user then enters the reference time shown on the clock generator. The value of this time is compared to the time value initially stored in a buffer, the difference is calculated, and the DOS clock is reset. Hitting any key will display the new PC system time. Occasionally this procedure must be repeated because of the offset caused by the 55ms steps in the PC clock.

Funding was provided by Office of Naval Research Grant N00014-91-J-1246.



## DOCUMENT LIBRARY

*Distribution List for Technical Report Exchange – May 5, 1994*

University of California, San Diego  
SIO Library 0175C (TRC)  
9500 Gilman Drive  
La Jolla, CA 92093-0175

Hancock Library of Biology & Oceanography  
Alan Hancock Laboratory  
University of Southern California  
University Park  
Los Angeles, CA 90089-0371

Gifts & Exchanges  
Library  
Bedford Institute of Oceanography  
P.O. Box 1006  
Dartmouth, NS, B2Y 4A2, CANADA

Commander  
International Ice Patrol  
1082 Shennecossett Road  
Groton, CT 06340-6095

NOAA/EDIS Miami Library Center  
4301 Rickenbacker Causeway  
Miami, FL 33149

Library  
Skidaway Institute of Oceanography  
10 Ocean Science Circle  
Savannah, GA 31411

Institute of Geophysics  
University of Hawaii  
Library Room 252  
2525 Correa Road  
Honolulu, HI 96822

Marine Resources Information Center  
Building E38-320  
MIT  
Cambridge, MA 02139

Library  
Lamont-Doherty Geological Observatory  
Columbia University  
Palisades, NY 10964

Library  
Serials Department  
Oregon State University  
Corvallis, OR 97331

Pell Marine Science Library  
University of Rhode Island  
Narragansett Bay Campus  
Narragansett, RI 02882

Working Collection  
Texas A&M University  
Dept. of Oceanography  
College Station, TX 77843

Fisheries-Oceanography Library  
151 Oceanography Teaching Bldg.  
University of Washington  
Seattle, WA 98195

Library  
R.S.M.A.S.  
University of Miami  
4600 Rickenbacker Causeway  
Miami, FL 33149

Maury Oceanographic Library  
Naval Oceanographic Office  
Building 1003 South  
1002 Balch Blvd.  
Stennis Space Center, MS 39522-5001

Library  
Institute of Ocean Sciences  
P.O. Box 6000  
Sidney, B.C. V8L 4B2  
CANADA

Library  
Institute of Oceanographic Sciences  
Deacon Laboratory  
Wormley, Godalming  
Surrey GU8 5UB  
UNITED KINGDOM

The Librarian  
CSIRO Marine Laboratories  
G.P.O. Box 1538  
Hobart, Tasmania  
AUSTRALIA 7001

Library  
Proudman Oceanographic Laboratory  
Bidston Observatory  
Birkenhead  
Merseyside L43 7 RA  
UNITED KINGDOM

IFREMER  
Centre de Brest  
Service Documentation - Publications  
BP 70 29280 PLOUZANE  
FRANCE

<b>REPORT DOCUMENTATION PAGE</b>	<b>1. REPORT NO.</b> WHOI-94-14	<b>2.</b>	<b>3. Recipient's Accession No.</b>
<b>4. Title and Subtitle</b> Advanced Engineering Laboratory Project Summaries 1991-1992			<b>5. Report Date</b> May 1994
			<b>6.</b>
<b>7. Author(s)</b> Edited by Daniel E. Frye			<b>8. Performing Organization Rept. No.</b> WHOI-94-14
<b>9. Performing Organization Name and Address</b>  Woods Hole Oceanographic Institution Woods Hole, Massachusetts 02543			<b>10. Project/Task/Work Unit No.</b>
			<b>11. Contract(C) or Grant(G) No.</b> (C) (G)
<b>12. Sponsoring Organization Name and Address</b>  Woods Hole Oceanographic Institution			<b>13. Type of Report &amp; Period Covered</b> Technical Report
			<b>14.</b>
<b>15. Supplementary Notes</b> This report should be cited as: Woods Hole Oceanog. Inst. Tech. Rept., WHOI-94-14.			
<b>16. Abstract (Limit: 200 words)</b>  The Advanced Engineering Laboratory of the Woods Hole Oceanographic Institution is a development laboratory within the Applied Ocean Physics and Engineering Department. Its function is the development of oceanographic instrumentation to test developing theories in oceanography, and to enhance current research projects in other disciplines within the community. This report summarizes recent and ongoing projects performed by members of this laboratory.			
<b>17. Document Analysis</b> <b>a. Descriptors</b> Advanced Engineering Laboratory electronic systems oceanographic instrumentation  <b>b. Identifiers/Open-Ended Terms</b>    <b>c. COSATI Field/Group</b>			
<b>18. Availability Statement</b>  Approved for public release; distribution unlimited.		<b>19. Security Class (This Report)</b> UNCLASSIFIED	<b>21. No. of Pages</b> 35
		<b>20. Security Class (This Page)</b>	<b>22. Price</b>